



Global relevance of atmospheric and land surface drivers for hot temperature extremes

Yigit Uckan^{1,2,3}, Melissa Ruiz-Vásquez^{1,2}, Kelley De Polt^{2,4}, René Orth^{1,2}

¹Faculty of Environment and Natural Resources, University of Freiburg, Freiburg, 79106, Germany

5 ²Department of Biogeochemical Integration, Max Planck Institute for Biogeochemistry, Jena, 07745, Germany

³School of Integrated Climate and Earth System Sciences, University of Hamburg, Hamburg, 20144, Germany

⁴Institute for Environmental Studies, Vrije Universiteit Amsterdam, Amsterdam, 1081 hv, the Netherlands

Correspondence to: Melissa Ruiz-Vásquez (mruiz@bgc-jena.mpg.de)

Abstract. Hot temperature extremes have severe impacts on society and ecosystems. Their magnitude and frequency are increasing with climate change in most regions globally. These extremes are driven by both atmospheric and land surface processes such as advection or reduced evaporative cooling. The contributions of the individual drivers to the formation and evolution of hot extremes have been analyzed in case studies for major past events, but the global relevance of drivers still remains unclear. In this study, we determine the relevance of (i) atmospheric drivers such as wind, geopotential height, geopotential height differences and surface net radiation, as well as (ii) land surface drivers such as evaporative fraction and enhanced vegetation index for hot extremes across the globe using observation-based data. Hot extremes are identified at daily and weekly time scales through the highest absolute temperature and an analogue-based approach to determine the relevance of the considered drivers. The results show that geopotential height at 500 hPa is overall the most relevant driver of hot extremes across the globe. Surface net radiation and enhanced vegetation index are the second most relevant drivers in many regions, particularly in tropical and semi-arid areas. We find that the relevance of land surface drivers is increasing within the studied period, and from daily to weekly durations. Revealing key regions and influential time scales of land surface drivers on hot extremes can inform more efficient prediction and management of the increasing threat these extremes pose.

1 Introduction

Hot extremes are events of severe weather characterized by prolonged periods of excessively high temperatures. These events pose significant risks to human health, agriculture, ecosystems, and infrastructure, making the understanding of their drivers a critical area of research (Anderegg et al., 2012, Goulart et al., 2021, Anderson & Bell, 2011, McEvoy et al., 2012). Moreover, because of the increasing trend of global temperatures, hot extremes have become longer, more frequent, and intense in recent years (Seneviratne et al., 2023).

Previous research on hot extremes has primarily focused on regional case studies to identify the drivers of specific events (Wehrli et al., 2019, Fischer et al., 2007). Studies such as Woollings et al. (2018) and Brunner et al. (2017) highlight the importance of atmospheric circulation patterns, such as blocking systems and jet stream anomalies, for the onset and



development of such events. On the other hand, land surface feedback mechanisms, including evaporative cooling deficits and vegetation water stress due to low soil moisture can exacerbate the hot extremes and lead to multi-hazard events (Wulff & Domeisen, 2019, Teuling et al., 2010, Miralles et al., 2014, Hauser et al., 2016). However, a joint and comparative assessment of these drivers is lacking such that also the relative importance of the land surface compared to that of atmospheric drivers is unclear (Perkins, 2015). Moreover, a global analysis to complement and reconcile the existing regional studies is missing (Sillmann et al., 2017). This limits our understanding regarding the physical mechanisms leading to hot extremes across the globe and our skill to forecast these events. We aim to address these knowledge gaps by conducting a global analysis where we determine and compare the relevance of atmospheric and land surface drivers of hot extremes. This includes the identification of relevant spatial patterns and regions of particular interest for each considered driver variable.

There is no one commonly accepted definition of hot extremes such that previous research has employed different temperature metrics or related indices and at different time scales (Perkins & Alexander, 2013, Brunner et al., 2017, Raha & Ghosh, 2020). In this context we define hot extremes through the highest absolute temperatures and consider daily and weekly time scales. Focusing on different time scales allows us to reveal to which extent the drivers of hot extremes, as well as the spatial patterns of their relevance, change with different durations of the events. Consequently, this can yield insights into potential differences of the mechanisms underlying the formation of hot extremes across time scales and regions.

2 Data and Methods

2.1 Data

For our definition of hot extremes, we use the 2 m daily mean temperature as this accounts for both day-time and night-time conditions. We make this choice because night-time temperatures play a role in the physiological response of plants to hot extremes (Wahid et al., 2007). Moreover, the increasing trend of night-time extreme temperatures also shows the relevance of using daily mean temperatures (Wu et al., 2023). As there is no common time scale for the definition of hot extremes, or more specifically heatwaves, we consider two different time scales, 1 day and 7 days. This will also allow testing to which extent the underlying drivers depend on the considered time scale. Further, we use the variables summarized in Table 1 to analyze different potential drivers of hot extremes globally. We classify the potential driver variables into two categories: atmospheric variables and land surface variables. These drivers are selected based on the existence of plausible physical pathways through which they can affect surface temperature.

Atmospheric variables include wind speed and geopotential height at three different atmospheric pressure levels which influence the distribution and movement of heat within the atmosphere (Xoplaki et al., 2003). Specifically, we analyze geopotential height and wind at three atmospheric levels: surface, 850 hPa, and 500 hPa. The selection of these three levels is based on their relevance to hot extremes formation and evolution, as well as findings from existing literature. The surface level can provide information about the advection of warm air (Jiménez-Esteve & Domeisen, 2022). The 850 hPa level, situated approximately 1.5 km above sea level, is used to assess lower-tropospheric processes. The 500 hPa level, roughly 5.5 km



above sea level, is often related to hot extremes formation due to blocking mechanisms at this level (Zschenderlein et al., 2019). This level is important for capturing mid-tropospheric patterns and the influence of large-scale atmospheric circulation
65 on weather systems (Ventura et al., 2023). In addition, we compute the geopotential height differences at 500 hPa pressure level for each grid cell with respect to the values in adjacent grid cells in the northern, eastern, southern and western directions. Land surface variables, such as evaporative fraction (EF), enhanced vegetation index (EVI), and surface net radiation, impact surface temperatures through the provision of energy, evaporative cooling as well as albedo which determines the amount of reflected solar energy (Seneviratne et al. 2010). EF is computed by normalizing evapotranspiration by surface net radiation.
70 It's important to mention that we compute EF using variables from two different datasets, which is justified as X-BASE uses ERA5 data in its formulation. We analyze the land surface variables across the same time scales considered for the hot extremes, but also at longer time scales in order to capture potential lagged effects arising from an accumulation of the influence of land surface variables over time. For example, for 1-day hot extreme events (Table 1; third column) we use values on the day of the event, an average of the variables on the event day and the 2 preceding days, as well as an average of the variables
75 on the event day and the 14 preceding days. Similarly for hot extremes of 7 days we consider time scales of 7, 14 and 28 days for the land surface variables. These time scales are important for understanding plant responses to hot extremes: water loss and stomatal closure are more pronounced on the daily time scale, while on the daily to weekly time scale vegetation is affected by leaf wilting and senescence (Zhang et al., 2016).
The spatial and temporal resolutions considered are 0.25 degrees and daily intervals, respectively for the study period of 2001
80 to 2020. In cases where the native resolutions of the datasets differed from these, the datasets were aggregated to a spatial resolution of 0.25 degrees and a daily temporal resolution using linear interpolation. Regarding the limited global coverage of the EF dataset, we mask grid cells without data, including deserts in Africa and Central Asia, in all considered datasets to ensure consistency in spatial coverage.

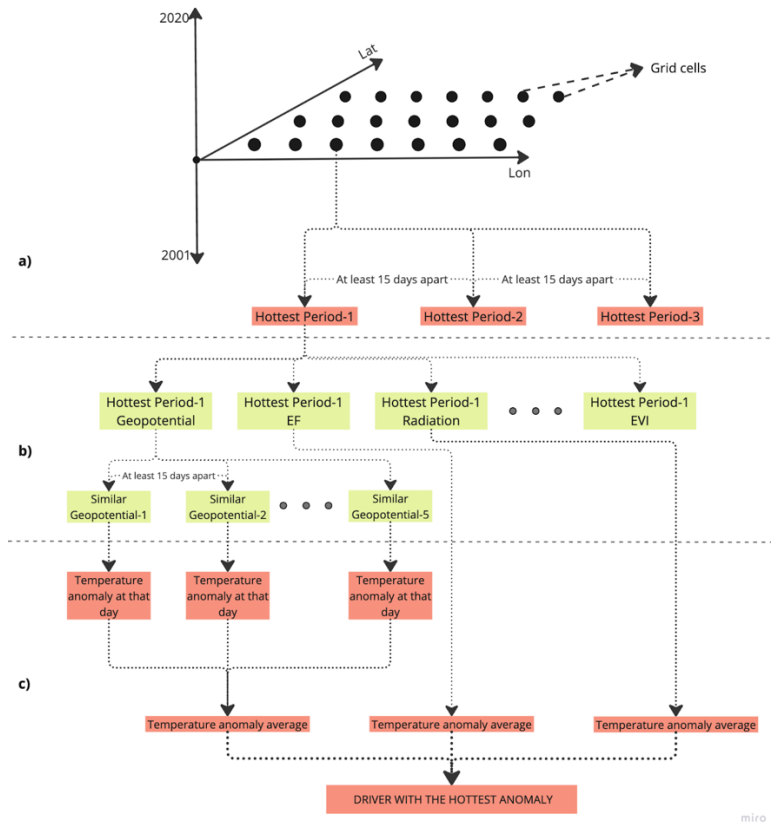


Table 1 Summary of considered driver variables

Variables	Source	1-day hot extremes	7-day hot extremes
Geopotential Height	ERA5 (Hersbach et al., 2020)	Pressure at the Surface	Pressure at the Surface
		Geopotential height at 850 hPa	Geopotential height at 850 hPa
		Geopotential height at 500 hPa	Geopotential height at 500 hPa
Wind Speed	ERA5 (Hersbach et al., 2020)	Wind at the Surface	Wind at the Surface
		Wind at 850 hPa	Wind at 850 hPa
		Wind at 500 hPa	Wind at 500 hPa
Geopotential Height Difference	ERA5 (Hersbach et al., 2020)	Geopotential height difference at 500 hPa	Geopotential height difference at 500 hPa
Enhanced Vegetation Index (EVI)	MODIS (Didan, 2015)	EVI 1-day	EVI 7-day
		EVI 3-day	EVI 14-day
		EVI 15-day	EVI 28-day
Evaporative Fraction (EF)	X-Base (Nelson et al., 2024)	EF 1-day	EF 7-day
	ERA5 (Hersbach et al., 2020)	EF 3-day	EF 14-day
		EF 15-day	EF 28-day
Surface Net Radiation	ERA5 (Hersbach et al., 2020)	Radiation 1-day	Radiation 7-day
		Radiation 3-day	Radiation 14-day
		Radiation 15-day	Radiation 28-day

2.2 Identification of hot extremes events

We identify the hot extreme events in each grid cell based on the highest absolute temperature values within our study period of 2001 to 2020. For the 7-day time scale we apply a moving average in order to remove variability from shorter time scales. For each type we select the three hottest events, ensuring that these are at least 15 days apart from each other and therefore independent, as shown in Fig. 1(a). The selected events occur during the warm seasons, as we pick the events with the highest temperatures.



95 **Figure 1** Workflow for determining main drivers of hot temperature extremes. (This figure is created by using miro.com)

2.3 Selection of analogues

After identifying hot extremes, we can determine the values of the considered driver variables for each event, and based on them we identify analogues as illustrated in Fig. 1(b). This means that for each driver and at each considered atmospheric level (i.e., geopotential height and wind) and temporal scale (i.e., EVI, EF, and surface net radiation) we select the five periods from the study period where values are the most similar to the originally investigated (Yiou et al. 2007). These analogues are only selected within a similar time of the year as the original hot extremes event to ensure comparable conditions; this is needed as e.g. circulation patterns with westerly winds from the North Atlantic tend to cool Europe in summer while warming it in winter. For this purpose, a 60-day window centered on the relevant hot extreme event is considered across all years to select the analogue periods. These periods are also at least 15 days apart from each other to ensure independence.

105 2.4 Determination of relevance of driver variables

Within the following step, shown in Fig. 1(c), we compute the temperature anomalies of the analogue periods identified for each driver. For each grid cell, we subtract the climatological mean temperature, from the temperature values recorded during



the analogue periods. This process is repeated for the second and third hottest periods in each grid cell, resulting in a total of 15 analogue periods for each driver variable. We then compute the mean across their temperature anomalies. This value is then an indicator of typical temperature anomalies associated with the specific conditions of each driver variable, and at the same time a measure of the relevance as a driver of the identified hot extremes. The main driver in a grid cell is then selected as the variable with the hottest mean temperature anomaly.

We then compare the mean temperature anomaly of the analogues with the mean temperature anomaly across the three considered hot extremes in each grid cell by calculating their ratio. This indicates the fraction of the actual temperature anomaly that can be explained with one driver, i.e. the degree of relevance of the dominant driver in the considered hot extreme events.

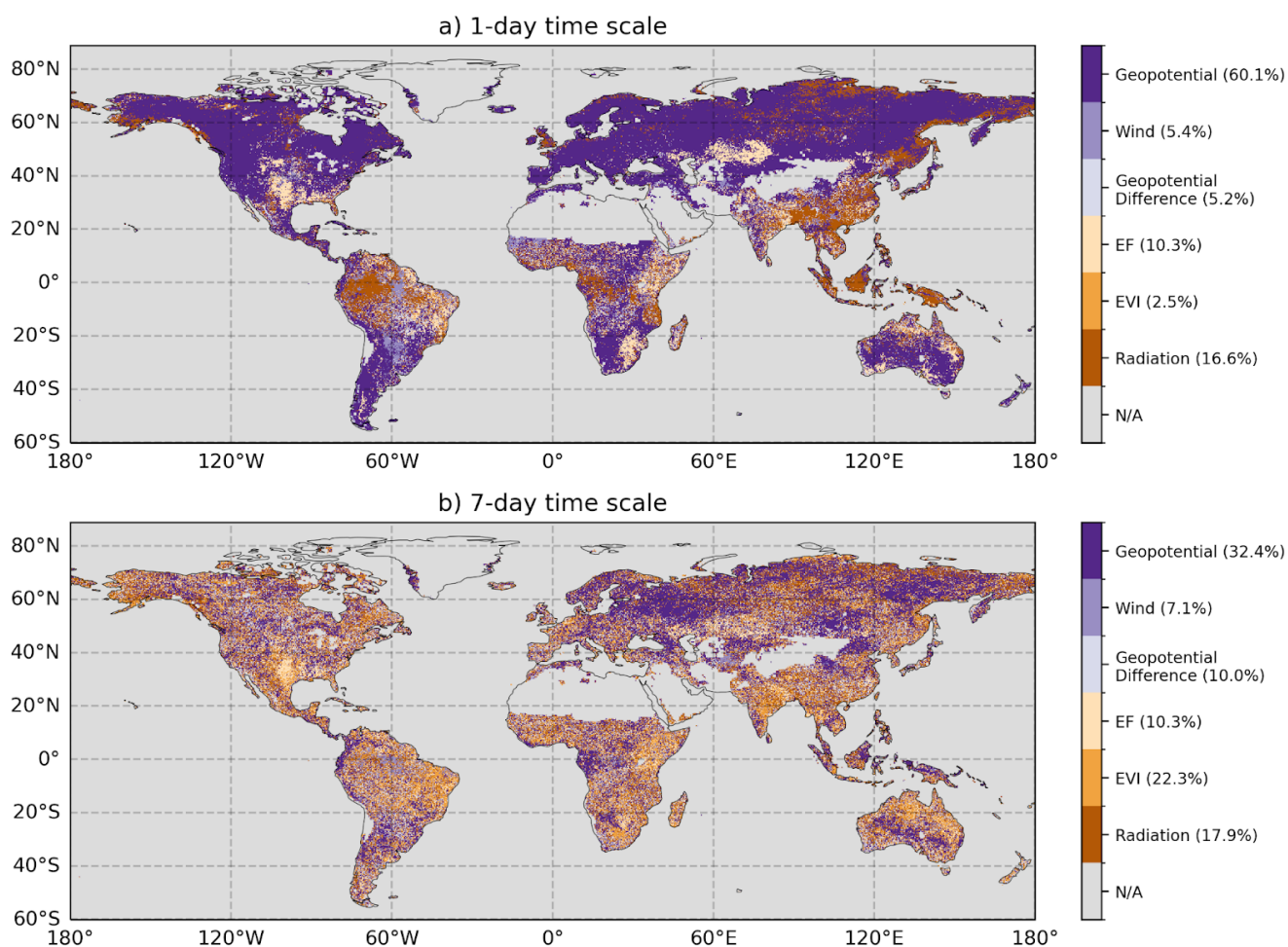
2.5 Effect of the increasing trend in hot temperatures extremes on the relevance of driver variables

In the light of the increasing trends in global temperature extremes (Seneviratne et al., 2023), we analyze potential changes in the relevance of the considered drivers of hot extremes over time. For this purpose, we divide the study period into two periods, 2001-2010 and 2011-2020, and employ the same methodology as described in Sections 2.1 to 2.4 to calculate the relevance of all driver variables for both time periods.



3 Results & Discussion

3.1 Global distribution of most relevant driver variables



125 **Figure 2** Dominant driver variables identified for 1-day and 7-day hot extremes. Fraction of study area where each driver is most influential is given in parentheses. The percentages indicated on the color bar reflect the proportion of the study area where hot extremes are most influenced by each variable.

The global distribution of the dominant variables for both 1-day and 7-day time scale extreme temperatures are illustrated within Fig. 2. The results are aggregated across geopotential height levels in the case of the atmospheric variables, and across time scales in the case of the land surface variables. The map corresponding to the 1-day time scale reveals that geopotential height is the predominant driver, accounting for approximately 60 % of the analyzed area. More specifically, the 500 hPa level geopotential height is most influential in mid-latitude regions. This finding supports existing literature that highlights the significant role of atmospheric blocking mechanisms in the formation of hot extremes in these latitudes and at 500 hPa pressure level (Pfahl & Wernli, 2012; Brunner et al., 2017; Jiménez-Esteve & Domeisen, 2022). Conversely, in primarily tropical

130



regions, surface net radiation substantially influences the occurrence of 1-day extreme temperature events. This can be
135 understood as lateral temperature and pressure gradients are weaker in the tropics such that atmospheric circulation is less
relevant while instead solar radiation is intense because of a larger and near-direct solar incident angle. Next to this, EF is
found to be the most relevant hot extremes driver across 10 % of the study area. This is particularly the case in Central North
America and Central Asia which are known as transition regions between wet and dry climate. In these regions
evapotranspiration and consequently evaporative cooling is relatively high but also limited by soil water availability which is
140 typically low during hot extremes (Koster, 2004; Wang et al., 2007). This way, reduced soil moisture and, as a result, lower
than usual EF leads to higher sensible heat flux, resulting in increased surface temperatures during hot extremes
(Schwingshackl et al., 2017; Teng et al., 2016). A more detailed depiction of drivers' relevances across height levels and time
scales is presented in Fig. A1.

For drivers of hot extremes at a time scale of 7 days we find that the relevance of land surface variables increases. Particularly
145 for EVI which is the most relevant driver in tropical or semi-arid warm regions, accounting for 22 % of the study area EVI
affects hot temperatures through the act of shading. In the identified regions where EVI is most relevant, temperatures can
reach levels at which leaves start to wilt which then reduces shading-related cooling and further amplifies the temperatures
(Brun et al., 2020). The role of EF is similar as observed for the 1-day time scale while net radiation is the dominant driver in
a slightly larger area which is also more shifted to high latitudes. This indicates that heat can accumulate through higher than
150 usual radiation persisting over some time (Miralles et al. 2014). Furthermore, land surface variables affect hot extremes mostly
at the same time scale of the hot extremes while lagged effects occur in few regions (Fig. A1). At the same time, geopotential
height remains the most dominant variable globally for 7-day hot extremes, while its relative influence is almost half of 1-day
hot extremes in mid-latitudes.

In order to analyze the spatial distribution of the dominant driver variables identified for 1-day and 7-day hot extremes with
155 respect to different land surface characteristics and climatic regimes, we employ a random forest approach where geopotential
height and EF serves as target variables while a range of hydro-climatological, vegetation and landscape variables is used as
predictors (Fig. A2). We find that long-term mean temperature and radiation are the most relevant predictor variables for both
1-day and 7-day hot extremes. Additionally, aridity (calculated as the ratio of long-term mean net radiation and unit-adjusted
long-term mean precipitation) and topography play a role while the other considered variables are less important. While
160 temperature has the highest relevance and is therefore selected as the primary variable, radiation, which ranks second in
relevance, is closely related to temperature as an atmospheric variable. To ensure the inclusion of a land-surface related factor,
we choose aridity, which captures the interaction between radiation and precipitation, thus providing a metric for assessing
land-surface influences on hot extremes.

The main driving variables of hot extremes, classified by temperature and aridity across different climatic regions, are shown
165 in Fig. 3. Geopotential height is most relevant across both cold and warm regions as well as dry and wet climate regimes. In
wet regions, radiation tends to be the second most relevant driver which is related to more intense solar radiation in the
respective tropical regions. Land surface variables EF and EVI are the second most important drivers in dry climate regimes,



and even the most relevant in semi-arid and warm climates. This is related to the fact that water availability is mostly just sufficient for vegetation in these regions which means that (i) it can supply significant evaporative cooling while (ii) during warm and dry conditions water availability will not be sufficient such that evaporative cooling decreases which in turn contributes to enhanced temperatures.

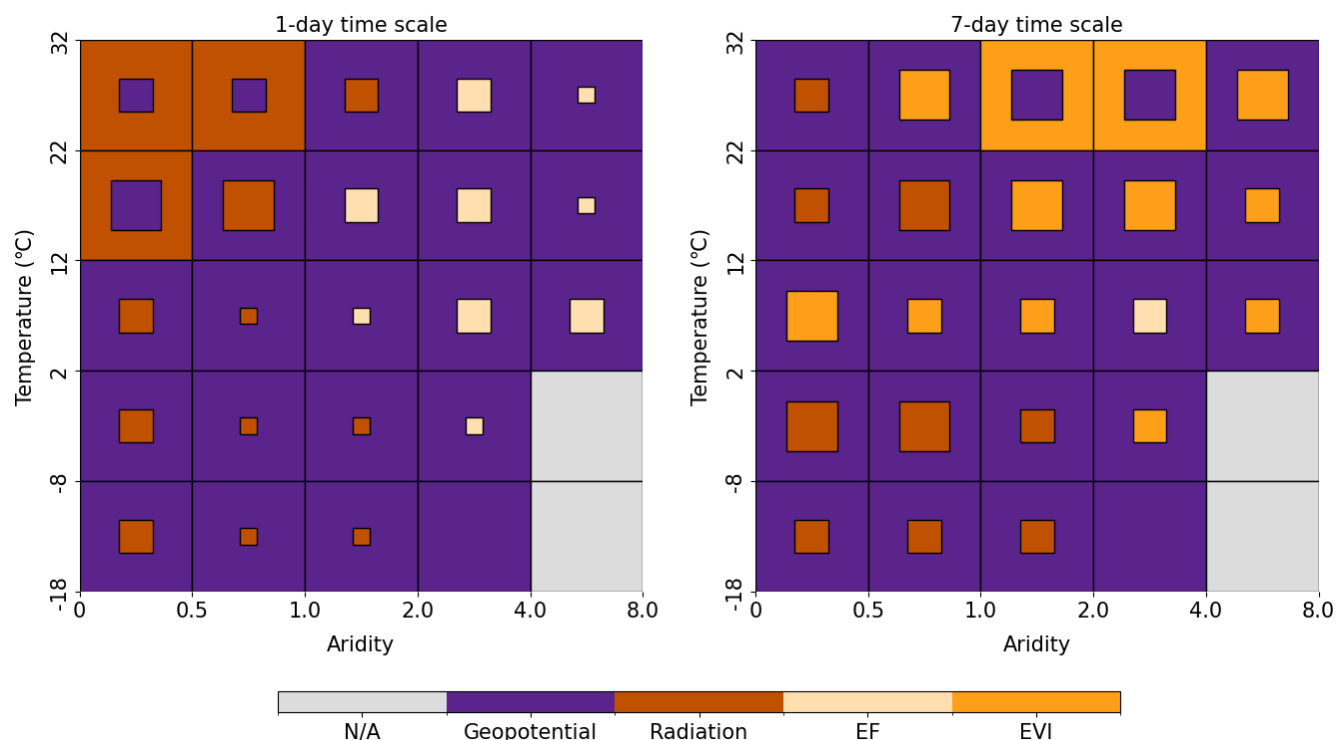


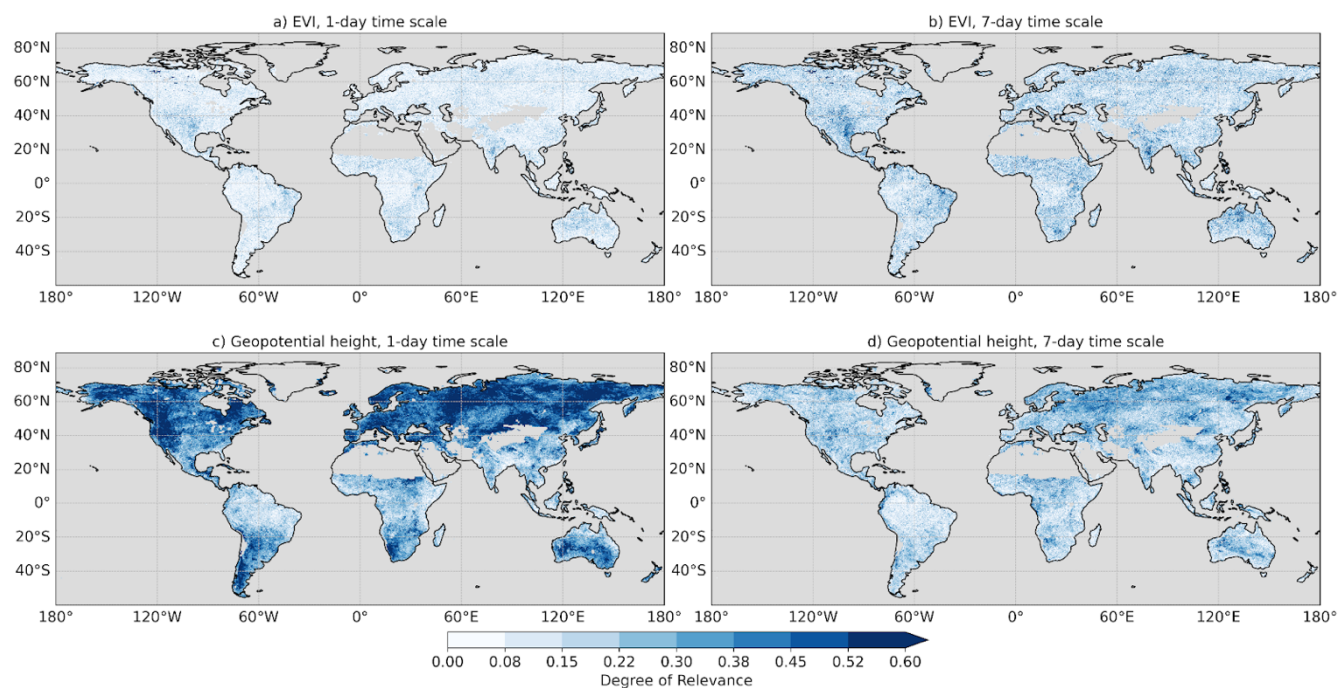
Figure 3 Main driving variables of hot extremes summarized across climate classes. Color of the boxes indicates which driver is most influential in the largest number of grid cells within the climate class. Color of the inner square indicates the second most relevant driver. The size of the square denotes the relative relevance of the second most important driver where large squares are used if the number of grid cells where the second most relevant driver is most influential exceeds 65 % of the number of grid cells where the most relevant driver is most influential. Likewise, medium-sized squares are used for fractions of 25 % - 65 % and small squares in the case of <25 %. Note that if there are fewer than 20 grid cells to represent the corresponding variables, the boxes will appear in gray or any other single color. Gray indicates that neither the first nor the second most dominant variables have enough grid cells, while any other single color indicates that only the first dominant variable has enough grid cells. The number of grid cells in each category is shown in Fig. A3.

These results have to be seen in the light of some limitations. The analogue methodology employed here does not account for interactions between the considered driver variables. This means that temperature anomalies associated with the analogues of a given variable could also partly result from anomalies in another variable that is closely connected to the first one and will hence add to its effect. We expect that the consideration of several hot extremes and of multiple analogues for each extreme for computation of the analogues can mitigate this problem as different weather and vegetation conditions characterize each of them. Furthermore, our main goal is to disentangle land surface and atmospheric drivers of hot extremes which are not expected to be strongly related to each other. Another limitation is the data quality of each driver variable. If there are lower signal-to-noise ratios for some considered variables than for others, this may affect the identification of analogues and related



190 temperature anomalies, and consequently the estimated relevance of the variable. Related to the consideration of several
geospheres within the set of our driver variables we have to rely on different data sources. At the same time we use established
products in this study which are all comprehensively validated and hence we expect that differences in data quality between
individual data streams is small.

3.2 Relative roles of the most important atmospheric and land surface drivers



195 **Figure 4** Degree of relevance of EVI (a, b) and geopotential height (c, d) at daily and weekly time scales. The degree of relevance is
computed as the ratio between the respective analogue temperature anomalies and the observed temperature anomalies during hot extremes.

In this section we analyze the main land surface and atmospheric drivers in more detail in terms of their degree of relevance
(i.e. the fraction of temperature anomalies of hot extremes explained by them according to the temperature anomalies of their
analogues). Fig. 4 presents the results for the Enhanced Vegetation Index (EVI) and geopotential height for 1-day and 7-day
200 hot extremes. Notably, the relevance of EVI increases with the time scale, in contrast to that of geopotential height, probably
due to the longer memory of land surface variables compared to the atmospheric variables (Mariotti et al., 2018). This also
relates with the substantial decrease in relevance of geopotential height towards hot extremes of from daily to week long time
scales. While EVI is the most relevant driver of hot extremes in more areas at longer time scales (Fig. 2), we find in the main
driving variables of hot extremes summarized across climate classes that it also exhibits a higher relevance in these areas but
205 also in other areas where other variables are even more important. This finding highlight that the land surface generally affects
hot extremes at longer time scales, as opposed to the more immediate influence of atmospheric drivers. This is related to the
fact that land surface effects such as evaporative cooling or shading are comparatively smaller but more persistent. Therefore



they are more influential at longer time scales and for hot extremes that build up during a time period without major changes in weather and air masses at a given location (Feldman et al., 2019; Dirmeyer et al., 2018; Sillmann et al., 2017).

210 Next, we summarize the results from the global degree of relevance of EVI and geopotential height in different climatic regions (Fig. A4). The results show that EVI is not only the dominant variable in semi-arid and arid regions, as shown in Fig. 3, but also it shows a relatively higher degree of relevance in those regions. On the other hand, geopotential height is more relevant in colder climates. These findings highlight that climate is the main modulator of the relevance of drivers of hot extremes across short to medium time scales.

215 Moreover we calculate the sum of the degree of relevance of the three most influential variables at each grid cell (Fig. A5). This shows which part of the observed hot temperature anomalies can be explained with our approach. The maps show that a large part of the observed hot temperature anomalies can be explained within the analogue approach. This suggests that we have included relevant and meaningful driver variables. At the same time the degree of relevance of the three most influential predictors is decreasing with increasing time scale. This is probably related to the increasing number of extreme heat drivers and their corresponding interactions that are relevant for longer-duration extreme heat events, such as synoptic-scale weather patterns and land surface conditions, as opposed to only micro- to mesoscale features like surface sensible heat fluxes (Domeisen et al., 2022). As the consideration of processes important for long-term prediction of extreme temperature, such as remote forcings, are outside the scope of this study, we do not consider time scales longer than 7 days. Note that in this calculation we do not jointly consider variables which are related to each other, i.e. geopotential height and geopotential height difference, or EVI and EF, such that we mitigate the effect of collinearities among the considered drivers. If such related variables are among the three most influential variables, we consider instead the next most relevant variable which is less related to the already considered variables.

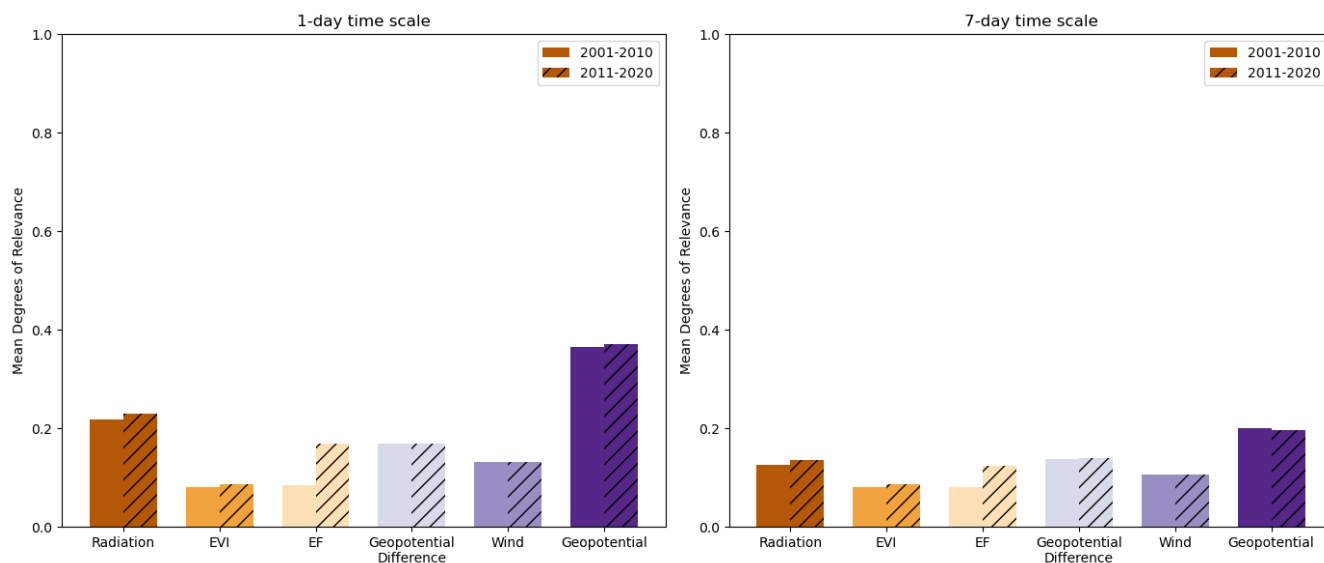
220
225

3.3 Trends in the relevance of drivers of hot extremes

The potential changes in the relevance of the considered drivers of hot extremes due to the positive trend in time of global temperatures in two periods: 2001-2010 and 2011-2020 are shown in Fig. 5. The main change we find is an increasing importance of EF. This is likely related to global increases of evapotranspiration in response to increased temperatures and precipitation in many regions (Douville et al. 2021). Higher evapotranspiration plays a more prominent role in the surface energy balance and hence also in modulating temperatures during hot extremes. At the same time, the relevance of geopotential height, radiation and wind slightly decrease. While the land surface becomes more relevant in driving hot extremes, the overall order of the relevance of drivers as shown in the primary analysis (Fig. 2) is not affected.

230
235

In addition to the global mean degree of relevance shown in Fig. 5, we calculate the area fraction where each driver is most relevant for inducing hot extremes (Fig. A6, Fig. A7). This confirms the results from Fig. 5 and shows that the area where EF is most relevant increases between both considered decades (Fig. A8). In turn, the area where geopotential height is most relevant is shrinking but remains larger than for any other considered driver.



240

Figure 5 Changes in the relevance of the considered hot extreme drivers between the first and second half of the study period. Bars without hatching denote results for the first half, and bars with hatching show results for the second half. Relevance is expressed as the mean degree of relevance across the study area.

4 Conclusions

245 This study provides a comprehensive analysis of the potential drivers of hot extremes, considering a wide selection of atmospheric and land surface variables. The results highlight that geopotential height, particularly at the 500 hPa level, is globally the dominant driver for hot extremes at the daily time scale, and especially influential in mid-latitude regions. This finding underscores the significant role of atmospheric blocking mechanisms in the formation of hot extremes. In contrast, surface net radiation is more influential in tropical regions, where it is more intense and can therefore exacerbate hot conditions.

250 Land surface variables, like evaporative fraction and enhanced vegetation index, influence hot extremes in transitional regions which are neither wet nor dry such that they can sustain significant evapotranspiration. Moreover, evapotranspiration depends on water availability such that soil moisture (i.e. land surface) variability influences evapotranspiration and consequently the surface energy balance and temperature (Denissen et al., 2024; Seneviratne et al., 2010).

255 These results complement the existing literature on drivers of hot extremes by jointly considering and comparing the relevance of atmospheric versus land surface drivers which were so far largely studied in isolation. Another novel aspect in our study is the consideration of hot extremes at different time scales. As this is not clearly defined in the literature, we decided to focus on daily and weekly time scales in order to analyze potential differences of drivers' relevances across time scales. We find that land surface variables such as the EVI and EF become more significant towards longer time scales. This highlights the importance of land-atmosphere interactions for the dynamics of hot extremes at increasing durations. It has been shown in a

260 case study, that hot extremes cause most impacts in terms of societal attention and public health at time scales between 2 weeks

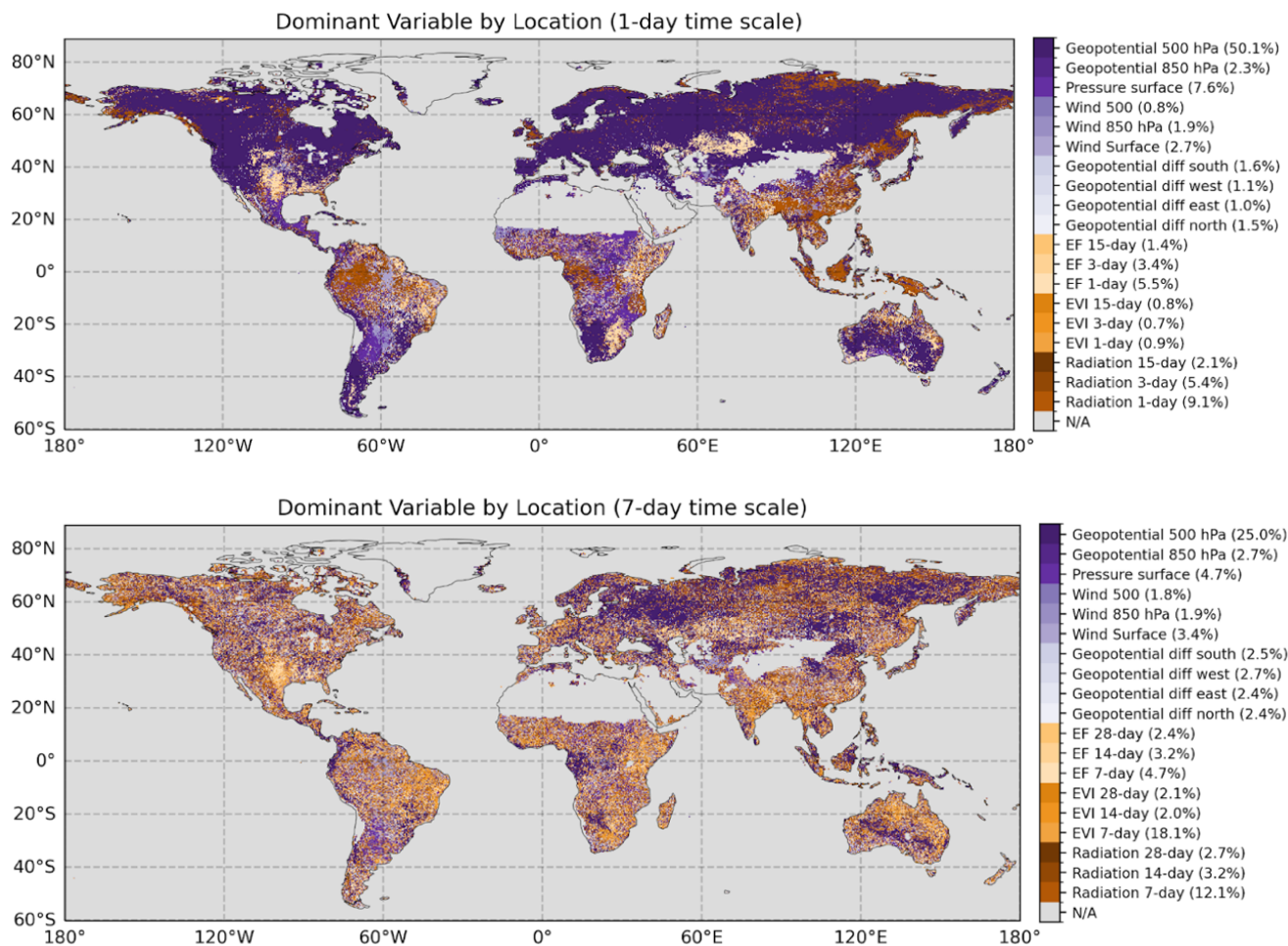


and 2 months (De Polt et al., 2023). This suggests that land surface drivers of hot extremes should regularly be included in related investigations as they are even more relevant towards these time scales. Also, this calls for even more comprehensive and multidisciplinary studies building upon our study to investigate and compare the relevance of drivers of hot extremes at weekly-monthly time scales and also to consider the role of the ocean and a larger scale spatial influence . This way, underlying mechanisms of hot extremes that cause most impacts could be better understood in order to inform forecasts and early warning systems.

Another interesting result of our study is the increasing relevance of the land surface in general and evaporative fraction in particular in driving hot extremes during the study period. This is likely related to higher temperatures and precipitation variability, which enhance the role of evaporation in the surface water and energy balances. Given the expected strong increases in the duration, magnitude, and frequency of hot extremes (Seneviratne et al., 2023), an accurate projection of the most affected regions and timing of these increases is essential. Our results highlight the importance of properly considering the land surface role in the onset and development of hot extremes, including vegetation dynamics to enable most accurate projections of these events. This way, our study motivates (i) further efforts to model the vegetation response to hydro-meteorological conditions at high spatial resolution where the coupling between vegetation and weather can be most accurately represented, as well as (ii) interest to monitor the root-zone soil moisture dynamics to better constrain vertical and lateral soil water movement in land surface models such that they can yield more accurate estimates of plant-available water.



Appendix A: Supplementary methods and results



280

Figure A1 Detailed dominant driver variables identified for 1-day and 7-day hot extremes. Percentage of the study area where each driver is most influential is given in parentheses.

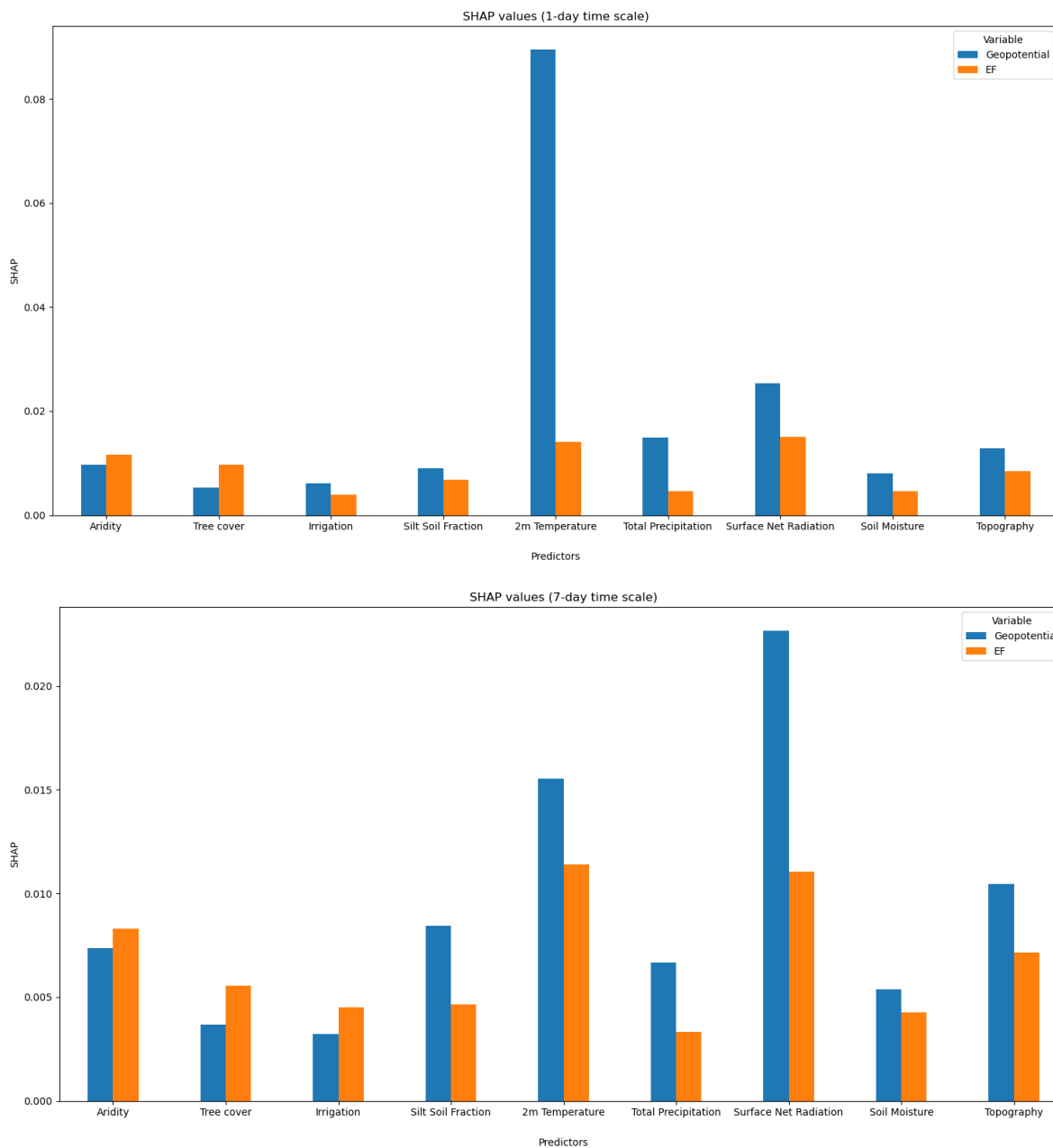


Figure A2 Relative importance (SHAP values) of multiple factors to explain the spatial patterns of geopotential height and EF as main drivers for 1-day and 7-day hot extremes.

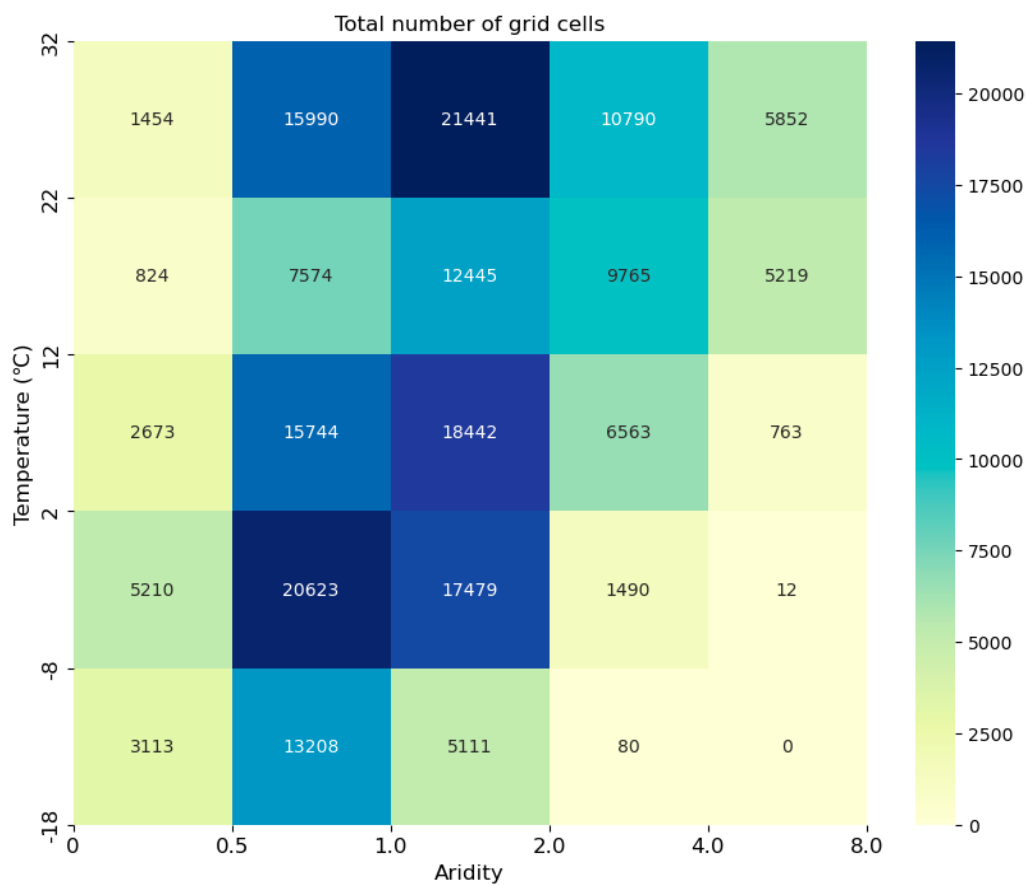


Figure A3 Total number of grid cells in each temperature-aridity category

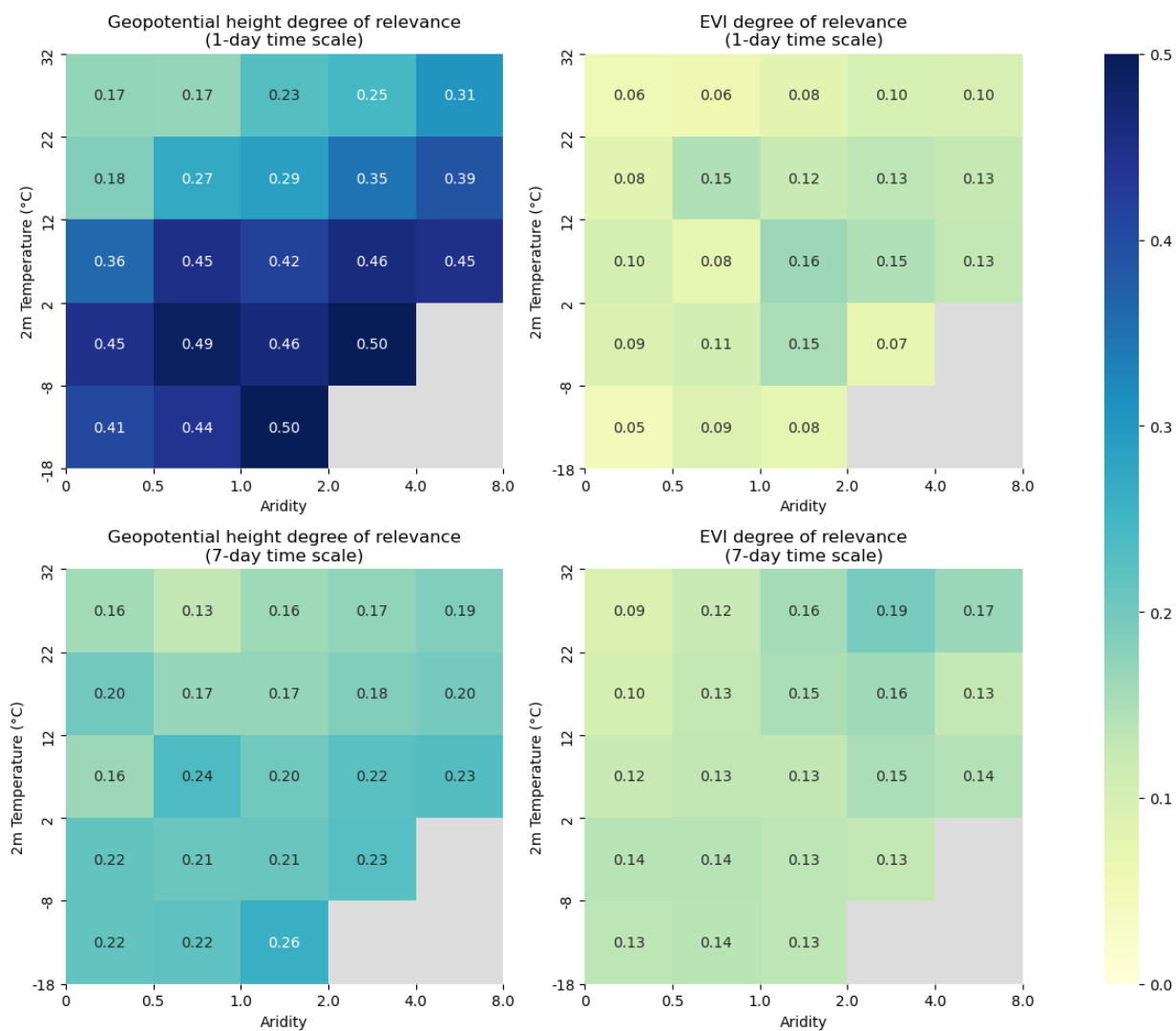


Figure A4 Geopotential height and EVI median degree of relevance summarized across climate classes (given by aridity and temperature ranges) for 1 and 7-day hot extremes. Gray indicates regions that are masked out due to insufficient number of grid cells (less than 20 grid cells)

290

295

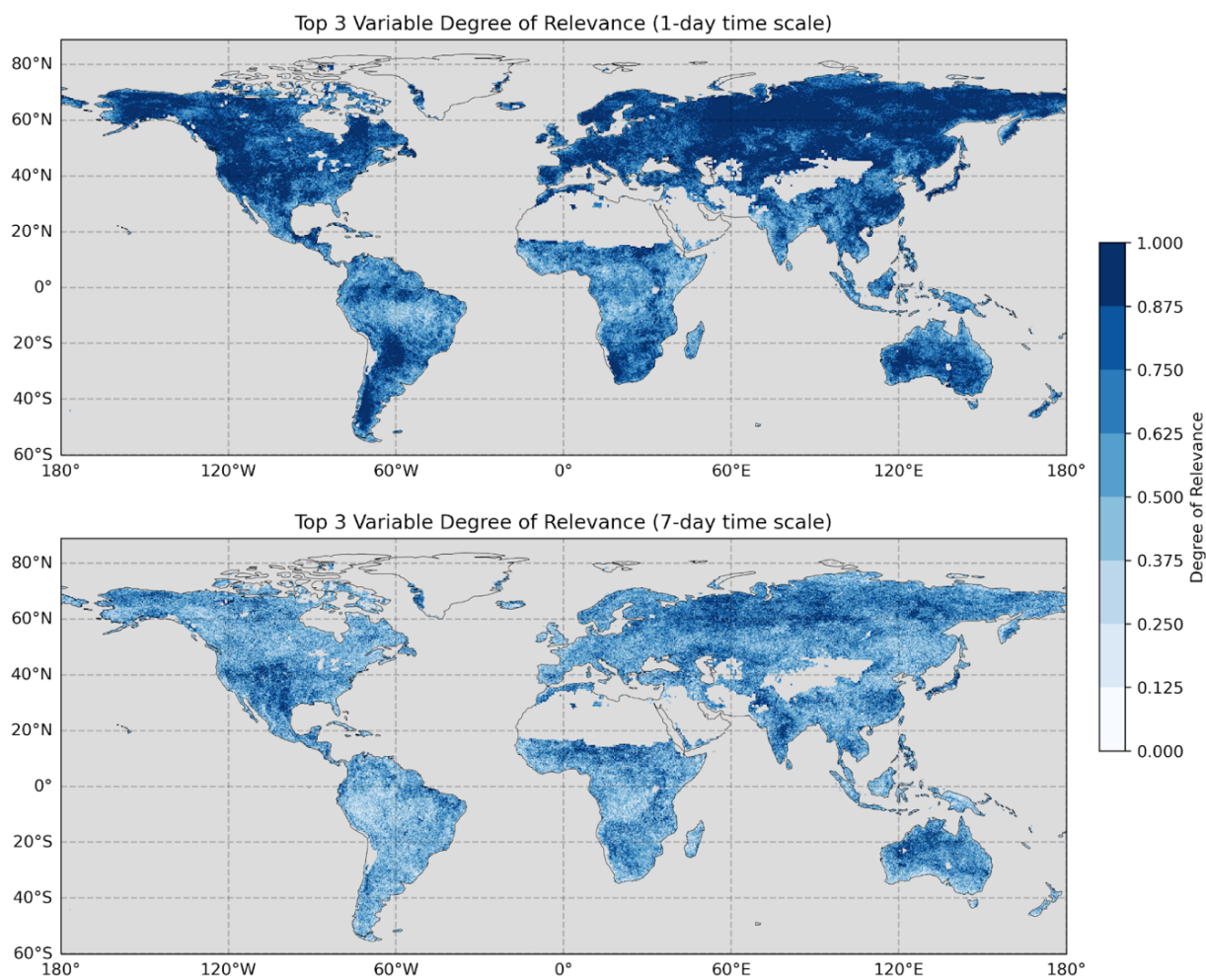


Figure A5 The sum of the degree of relevance of the three most influential variables for 1-day and 7-day hot extremes. Gray color indicates ocean/inland water or grid cells with insufficient data.

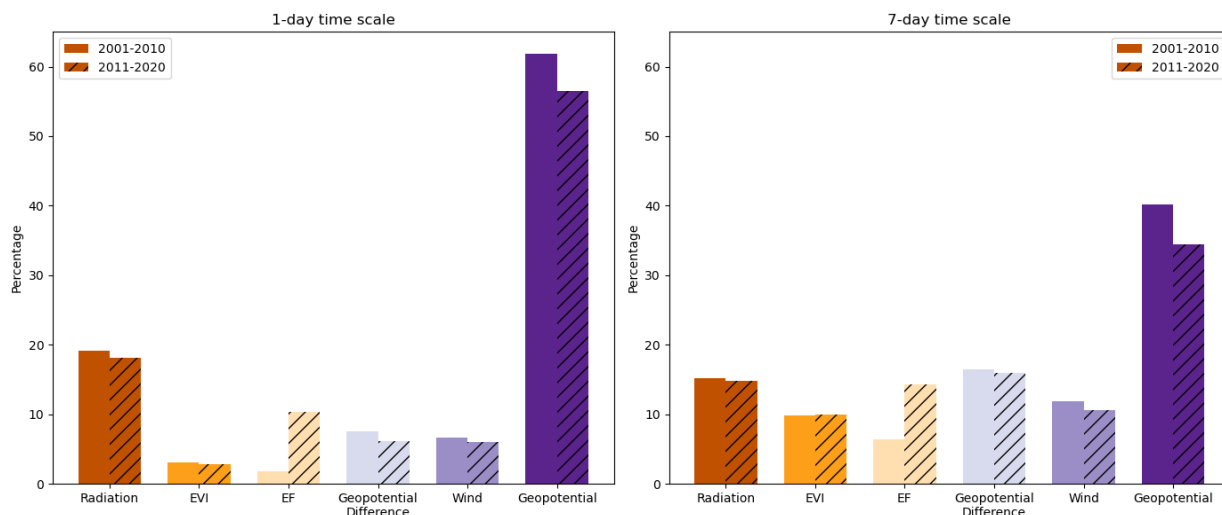


Figure A6 Similar to figure 5 but relevance is expressed as the percentage of the study area where each driver is found to be the most relevant.

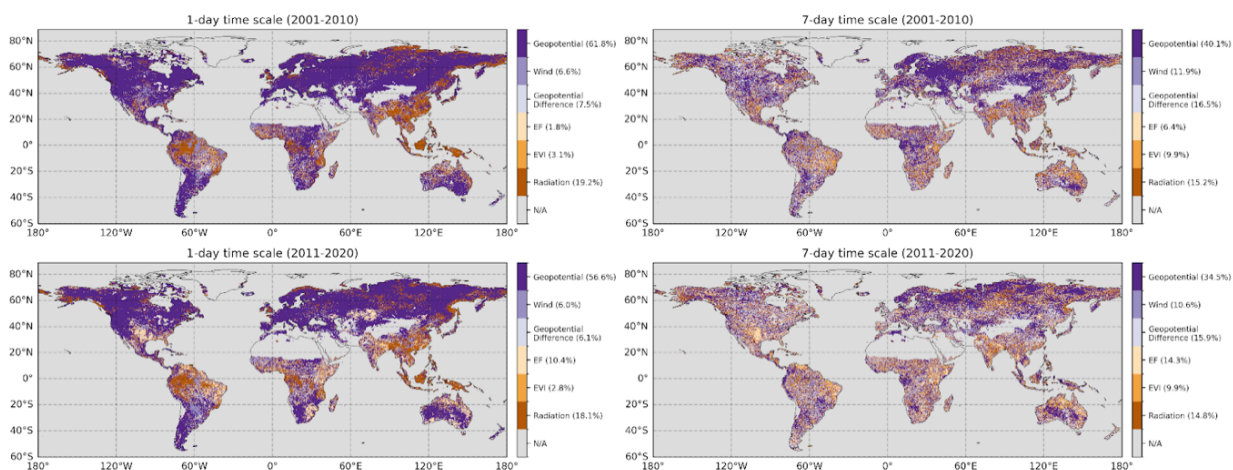


Figure A7 Dominant driver variables identified for 1-day and 7-day hot extremes over the time periods 2001-2010 (first row) and 2011-2020 (second row). Percentage of the study area where each driver is most influential is given in parentheses.

305

310



Figure A8 The median EF degree of relevance, categorized by aridity index and 2 m temperature ranges, across two time periods (2001-2010 and 2011-2020) and two temporal resolutions (1-day and 7-day). Gray indicates regions that are masked out due to insufficient number of grid cells (less than 20 grid cells)

315



Code and data availability

The variables from ERA5 are available at <https://cds-beta.climate.copernicus.eu/datasets/reanalysis-era5-complete?tab=overview> (Hersbach et al., 2020). The EVI data from MODIS is available through NASA's data catalogue at <https://lpdaac.usgs.gov/products/mod13c1v006/> (Didan, 2015). FLUXCOM-X-BASE evapotranspiration data is available at https://meta.icos-cp.eu/collections/_185vWiIV81AifoxCkty50YI (Nelson et al., 2024).

Author contributions

YU, MRV, RO jointly designed the study. YU performed the computations, plots and data analysis. MRV contributed with coding support and data acquisition. YU, MRV, KDP, RO contributed to the discussion and interpretation of the results, writing of the paper.

Competing interests

The authors declare that they have no conflict of interest.

Acknowledgments

The authors express their gratitude to Ulrich Weber for his assistance with data retrieval and processing, and to the Hydrology-Biosphere-Climate Interactions group at the Max Planck Institute for Biogeochemistry for their valuable contributions. Melissa Ruiz-Vásquez and Kelley De Polt acknowledge support from the International Max Planck Research School for Global Biogeochemical Cycles (IMPRS). René Orth was supported by the German Research Foundation (Emmy Noether grant no. 391059971)

References

Anderegg, W. R. L., Kane, J. M., & Anderegg, L. D. L.: Consequences of widespread tree mortality triggered by drought and temperature stress. *Nat Clim Change*, 3(1), 30–36, <https://doi.org/10.1038/nclimate1635>, 2012.

Anderson, G. B., & Bell, M. L.: Heat Waves in the United States: Mortality Risk during Heat Waves and Effect Modification by Heat Wave Characteristics in 43 U.S. Communities. *Environ Health Persp*, 119(2), 210–218, <https://doi.org/10.1289/ehp.1002313>, 2011.



- Brun, P., Psomas, A., Ginzler, C., Thuiller, W., Zappa, M., & Zimmermann, N. E.: Large-scale early-wilting response of Central European forests to the 2018 extreme drought. *Glob Change Biol*, 26(12), 7021–7035, <https://doi.org/10.1111/gcb.15360>, 2020.
- Brunner, L., Hegerl, G. C., & Steiner, A. K.: Connecting Atmospheric Blocking to European Temperature Extremes in Spring. *J Climate*, 30(2), 585–594, <https://doi.org/10.1175/jcli-d-16-0518.1>, 2017.
- 345 De Polt, K., Ward, P. J., de Ruiter, M., Bogdanovich, E., Reichstein, M., Frank, D., & Orth, R.: Quantifying impact-relevant heatwave durations. *Environ Res Lett*, 18(10), 104005–104005, <https://doi.org/10.1088/1748-9326/acf05e>, 2023.
- Denissen, J. M. C., Teuling, A. J., Sujun Koirala, Reichstein, M., Balsamo, G., Vogel, M. M., Yu, X., & Orth, R.: Intensified future heat extremes linked with increasing ecosystem water limitation. *Earth Syst Dynam*, 15(3), 717–734, <https://doi.org/10.5194/esd-15-717-2024>, 2024.
- 350 Didan K.: MOD13C1 MODIS/Terra Vegetation Indices 16-Day L3 Global 0.05Deg CMG V006. NASA EOSDIS Land Processes Distributed Active Archive Center, <https://doi.org/10.5067/MODIS/MOD13C1.006>, 2015.
- Dirmeyer, P. A., Chen, L., Wu, J., Chee Mahn Shin, Huang, B., Cash, B. A., Bosilovich, M. G., Sarith Mahanama, Koster, R. D., Santanello, J. A., Ek, M., Balsamo, G., Dutra, E., & Lawrence, D. M.: Verification of Land–Atmosphere Coupling in *Forecast Models, Reanalyses, and Land Surface Models Using Flux Site Observations*. *J Hydrometeorol*, 19(2), 375–392, <https://doi.org/10.1175/jhm-d-17-0152.1>, 2018.
- 355 Domeisen, D. I. V., Eltahir, E. A. B., Fischer, E. M., Knutti, R., Perkins-Kirkpatrick, S. E., Schär, C., Seneviratne, S. I., Weisheimer, A., & Wernli, H.: Prediction and projection of heatwaves. *Nature Reviews Earth & Environment*, 36(50), <https://doi.org/10.1038/s43017-022-00371-z>, 2022.
- 360 Douville, H., K. Raghavan, J. Renwick, R.P. Allan, P.A. Arias, M. Barlow, R. Cerezo-Mota, A. Cherchi, T.Y. Gan, J. Gergis, D. Jiang, A. Khan, W. Pokam Mba, D. Rosenfeld, J. Tierney, and O. Zolina: Water Cycle Changes. In *Climate Change 2021: The Physical Science Basis. Contribution of Working Group I to the Sixth Assessment Report of the Intergovernmental Panel on Climate Change* [Masson-Delmotte, V., P. Zhai, A. Pirani, S.L. Connors, C. Péan, S. Berger, N. Caud, Y. Chen, L. Goldfarb, M.I. Gomis, M. Huang, K. Leitzell, E. Lonnoy, J.B.R. Matthews, T.K. Maycock, T. Waterfield, O. Yelekçi, R. Yu, and B. Zhou (eds.)]. Cambridge University Press, Cambridge, United Kingdom and New York, NY, USA, pp. 1055–1210, doi:10.1017/9781009157896.010, 2021.
- 365 Feldman, A. F., Short Gianotti, D. J., Trigo, I. F., Salvucci, G. D., & Entekhabi, D.: Satellite-Based Assessment of Land Surface Energy Partitioning–Soil Moisture Relationships and Effects of Confounding Variables. *Water Resour Res*, 55(12), 10657–10677, <https://doi.org/10.1029/2019wr025874>, 2019.
- 370 Fischer, E. M., Seneviratne, S. I., Lüthi, D., & Schär, C.: Contribution of land-atmosphere coupling to recent European summer heat waves. *Geophys Res Lett*, 34(6), <https://doi.org/10.1029/2006gl029068>, 2007.
- Goulart, H. M. D., van der Wiel, K., Folberth, C., Balkovic, J., & van den Hurk, B.: Storylines of weather-induced crop failure events under climate change. *EARTH SYST DYNAM*, 12(4), 1503–1527, <https://doi.org/10.5194/esd-12-1503-2021>, 2021.



- Hauser, M., Orth, R., & Seneviratne, S. I.: Role of soil moisture versus recent climate change for the 2010 heat wave in western
375 Russia. *Geophys. Res. Lett.*, 43(6), 2819–2826, <https://doi.org/10.1002/2016gl068036>, 2016.
- Hersbach, H., Bell, B., Berrisford, P., Hirahara, S., Horányi, A., Muñoz-Sabater, J., Nicolas, J., Peubey, C., Radu, R., Schepers,
D., Simmons, A., Soci, C., Abdalla, S., Abellan, X., Balsamo, G., Bechtold, P., Biavati, G., Bidlot, J., Bonavita, M., & Chiara,
G.: The ERA5 global reanalysis. *Q J Roy Meteor Soc.*, 146(730), <https://doi.org/10.1002/qj.3803>, 2020.
- Jiménez-Esteve, B., & Domeisen, Daniela. I. V.: The role of atmospheric dynamics and large-scale topography in driving
380 heatwaves. *Q J Roy Meteor Soc.*, <https://doi.org/10.1002/qj.4306>, 2022.
- Koster, R. D.: Regions of Strong Coupling Between Soil Moisture and Precipitation. *Science*, 305(5687), 1138–1140,
<https://doi.org/10.1126/science.1100217>, 2004.
- Mariotti, A., Ruti, P. M., & Rixen, M.: Progress in subseasonal to seasonal prediction through a joint weather and climate
community effort. *NPJ Climate and Atmospheric Science*, 1(1), <https://doi.org/10.1038/s41612-018-0014-z>, 2018.
- 385 McEvoy, D., Ahmed, I., & Mullett, J.: The impact of the 2009 heat wave on Melbourne’s critical infrastructure. *Local
Environment*, 17(8), 783–796, <https://doi.org/10.1080/13549839.2012.678320>, 2012.
- Miralles, D. G., Teuling, A. J., van Heerwaarden, C. C., & Vilà-Guerau de Arellano, J.: Mega-heatwave temperatures due to
combined soil desiccation and atmospheric heat accumulation. *Nat Geosci*, 7(5), 345–349, <https://doi.org/10.1038/ngeo2141>,
2014
- 390 Nairn, J., & Fawcett, R.: The Excess Heat Factor: A Metric for Heatwave Intensity and Its Use in Classifying Heatwave
Severity. *Int J Env Res Pub He*, 12(1), 227–253, <https://doi.org/10.3390/ijerph120100227>, 2014.
- Nelson, J. A., Walther, S., Gans, F., Kraft, B., Weber, U., Novick, K., Buchmann, N., Mirco Migliavacca, Wohlfahrt, G.,
Ladislav Šigut, Ibrom, A., Papale, D., Mathias Göckede, Duveiller, G., Knohl, A., Lukas Hörtnagl, Scott, R. L., Zhang, W.,
Zayd Mahmoud Hamdi, & Reichstein, M.: X-BASE: the first terrestrial carbon and water flux products from an extended data-
395 driven scaling framework, FLUXCOM-X. *EGUsphere [Preprint]*, <https://doi.org/10.5194/egusphere-2024-165>, 2024.
- Perkins, S. E.: A review on the scientific understanding of heatwaves—Their measurement, driving mechanisms, and changes
at the global scale. *Atmos Res*, 164-165, 242–267, <https://doi.org/10.1016/j.atmosres.2015.05.014>, 2015.
- Perkins, S. E., & Alexander, L. V.: On the Measurement of Heat Waves. *J Climate*, 26(13), 4500–4517,
<https://doi.org/10.1175/jcli-d-12-00383.1>, 2013.
- 400 Pfahl, S., & Wernli, H.: Quantifying the relevance of atmospheric blocking for co-located temperature extremes in the Northern
Hemisphere on (sub-)daily time scales. *Geophys Res Lett*, 39(12), <https://doi.org/10.1029/2012gl052261>, 2012.
- Raha, S., & Ghosh, S. K.: Heatwave duration: Characterizations using probabilistic inference. *Environmetrics/EnvironMetrics*,
31(5), <https://doi.org/10.1002/env.2626>, 2020.
- Schwingshackl, C., Hirschi, M., & Seneviratne, S. I.: Quantifying Spatiotemporal Variations of Soil Moisture Control on
405 Surface Energy Balance and Near-Surface Air Temperature. *J Climate*, 30(18), 7105–7124, <https://doi.org/10.1175/jcli-d-16-0727.1>, 2017.



- Seneviratne, S. I., Corti, T., Davin, E. L., Hirschi, M., Jaeger, E. B., Lehner, I., Orlowsky, B., & Teuling, A. J.: Investigating soil moisture–climate interactions in a changing climate: A review. *Earth-Sci Rev*, 99(3-4), 125–161, <https://doi.org/10.1016/j.earscirev.2010.02.004>, 2010.
- 410 Seneviratne, S. I., Zhang, X., Adnan, M., Badi, W., Dereczynski, C., Luca, A. D., Ghosh, S., Iskandar, I., Kossin, J., Lewis, S., Otto, F., Pinto, I., Satoh, M., Vicente-Serrano, S. M., Wehner, M., & Zhou, B.: Weather and climate extreme events in a changing climate. In V. Masson-Delmotte, P. Zhai, A. Pirani, S. L. Connors, C. Péan, S. Berger, N. Caud, Y. Chen, L. Goldfarb, M. I. Gomis, M. Huang, K. Leitzell, E. Lonnoy, J. B. R. Matthews, T. K. Maycock, T. Waterfield, O. Yelekçi, R. Yu, & B. Zhou (Eds.), *Climate change 2021: The physical science basis. Contribution of Working Group I to the Sixth Assessment*
- 415 *Report of the Intergovernmental Panel on Climate Change* (pp. 1513-1766). Cambridge University Press, <https://doi.org/10.1017/9781009157896.013>, 2023.
- Sillmann, J., Thorarinsdottir, T., Keenlyside, N., Schaller, N., Alexander, L. V., Hegerl, G., Seneviratne, S. I., Vautard, R., Zhang, X., & Zwiers, F. W.: Understanding, modeling and predicting weather and climate extremes: Challenges and opportunities. *Weather and Climate Extremes*, 18, 65–74, <https://doi.org/10.1016/j.wace.2017.10.003>, 2017.
- 420 Teng, H., Branstator, G., Meehl, G. A., & Washington, W. M.: Projected intensification of subseasonal temperature variability and heat waves in the Great Plains. *Geophys Res Lett*, 43(5), 2165–2173, <https://doi.org/10.1002/2015gl067574>, 2016.
- Teuling, A. J., Seneviratne, S. I., Stöckli, R., Reichstein, M., Moors, E., Ciais, P., Luysaert, S., van den Hurk, B., Ammann, C., Bernhofer, C., Dellwik, E., Gianelle, D., Gielen, B., Grünwald, T., Klumpp, K., Montagnani, L., Moureaux, C., Sottocornola, M., & Wohlfahrt, G.: Contrasting response of European forest and grassland energy exchange to heatwaves. *Nat*
- 425 *Geosci*, 3(10), 722–727, <https://doi.org/10.1038/ngeo950>, 2010.
- Ventura, S., Josep Ramon Miró, Juan Carlos Peña, & Villalba, G.: Analysis of synoptic weather patterns of heatwave events. *Clim Dynam*, 61(9-10), 4679–4702, <https://doi.org/10.1007/s00382-023-06828-1>, 2023.
- Wahid, A., Gelani, S., Ashraf, M., & Foolad, M. R.: Heat tolerance in plants: An overview. *Environ Exp Bot*, 61(3), 199–223, <https://doi.org/10.1016/j.envexpbot.2007.05.011>, 2007.
- 430 Wang, G., Kim, Y., & Wang, D.: Quantifying the Strength of Soil Moisture–Precipitation Coupling and Its Sensitivity to Changes in Surface Water Budget. *J Hydrometeorol*, 8(3), 551–570, <https://doi.org/10.1175/jhm573.1>, 2007.
- Wehrli, K., Guillod, B. P., Hauser, M., Leclair, M., & Seneviratne, Sonia I.: Identifying Key Driving Processes of Major Recent Heat Waves. *J Geophys Res-Atmos*, 124(22), 11746–11765, <https://doi.org/10.1029/2019jd030635>, 2019.
- Woollings, T., Barriopedro, D., Methven, J., Son, S.-W., Martius, O., Harvey, B., Sillmann, J., Lupo, A. R., & Seneviratne, S.: Blocking and its Response to Climate Change. *Current Climate Change Reports*, 4(3), 287–300, <https://doi.org/10.1007/s40641-018-0108-z>, 2018.
- 435 Wu, S., Luo, M., Zhao, R., Li, J., Sun, P., Liu, Z., Wang, X., Wang, P., & Zhang, H.: Local mechanisms for global daytime, nighttime, and compound heatwaves. *Npj Climate and Atmospheric Science*, 6(1), 1–13, <https://doi.org/10.1038/s41612-023-00365-8>, 2023.



- 440 Wulff, C. O., & Domeisen, D. I. V.: Higher Subseasonal Predictability of Extreme Hot European Summer Temperatures as Compared to Average Summers. *Geophys Res Lett*, 46(20), 11520–11529, <https://doi.org/10.1029/2019gl084314>, 2019.
- Xoplaki, E., González-Rouco, J. F., Luterbacher, J., & Wanner, H.: Mediterranean summer air temperature variability and its connection to the large-scale atmospheric circulation and SSTs. *Clim Dynam*, 20(7-8), 723–739, <https://doi.org/10.1007/s00382-003-0304-x>, 2003.
- 445 Yiou, P., Vautard, R., Naveau, P., & Cassou, C.: Inconsistency between atmospheric dynamics and temperatures during the exceptional 2006/2007 fall/winter and recent warming in Europe. *Geophys Res Lett*, 34(21), <https://doi.org/10.1029/2007gl031981>, 2007.
- Zhang, Y., Xiao, X., Zhou, S., Philippe Ciais, McCarthy, H., & Luo, Y.: Canopy and physiological controls of GPP during drought and heat wave. *Geophys Res Lett*, 43(7), 3325–3333, <https://doi.org/10.1002/2016gl068501>, 2016.
- 450 Zschenderlein, P., Fink, A. H., Pfahl, S., & Wernli, H.: Processes determining heat waves across different European climates. *Q J Roy Meteor Soc*, 145(724), 2973–2989, <https://doi.org/10.1002/qj.3599>, 2019.